RELATIONSHIP BETWEEN PRESYNAPTIC CALCIUM CURRENT AND POSTSYNAPTIC POTENTIAL IN SQUID GIANT SYNAPSE

R. LLINÁS, I. Z. STEINBERG, AND K. WALTON, *Department of Physiology and Biophysics, New York University Medical Center, New York 10016, and Department of Chemical Physics, Weizmann Institute of Science, Rehovot, Israel*

ABSTRACT The relation between calcium current and transmitter release was studied in squid giant synapse. It was found that the voltage-dependent calcium current triggers the release of synaptic transmitter in direct proportion to its magnitude and duration. Transmitter release occurs with a delay of ~200 μs after the influx of calcium. A model is presented which describes these relations formally.

INTRODUCTION

In conjunction with the wealth of results obtained over the last decade in the muscle endplate (cf. Steinbach and Stevens, 1976), investigation of the transmission properties in the squid giant synapse (Young, 1939) has provided major insights into the nature of the depolarization-release coupling which characterizes chemical synaptic transmission (cf. Katz, 1969). Specifically, the squid giant synapse allowed the direct and simultaneous study of the pre- and postsynaptic electrophysiological changes underlying the transmission phenomena (Bullock and Hagiwara, 1957; Hagiwara and Tasaki, 1958; Takeuchi and Takeuchi, 1962; Miledi and Slater, 1966). The pharmacological blockage of the sodium and potassium conductances further aided in this endeavor by allowing transmission to be studied in the absence of action potentials (Bloedel et al., 1966; Katz and Miledi, 1967; Kusano et al., 1967) and, in particular, it revealed the presence at the presynaptic terminal of a calcium conductance which could become self-regenerative after a reduction of the voltage-dependent potassium conductance (Katz and Miledi, 1969; Llinás and Nicholson, 1975). This research gave further impetus to the calcium hypothesis of synaptic release (cf. Katz, 1969).

The actual occurrence of an inward calcium flux, capable of producing an increase in intracellular ionized calcium ($[Ca^{2+}]_i$) during synaptic transmission, was then identified by intracellular injection of the photoreactive protein aequorin into the presynaptic terminal in the squid giant synapse (Llinás and Nicholson, 1975); however, it was not until recently that voltage clamp studies demonstrated and characterized a calcium current in this preterminal (Llinás et al., 1976). In the accompanying paper (Llinás et al., 1981) we have described the time and voltage dependence of this presynaptic current and presented a kinetic model which proposes specific parameters for the calcium channel. The main thrust of the present paper will be the quantitative analysis of the relationship between the presynaptic calcium current

(I_{Ca}) and the postsynaptic response (EPSP). While the postsynaptic response itself is not a completely accurate indicator of transmitter release, it is possible, using this measurement, to approximate the time course and amount of transmitter released by a given presynaptic I_{Ca}. As will be seen later, this relationship is quite complex and assumptions regarding the existence and characteristics of several sequential steps in the release process must be made. These steps include the diffusion of calcium into the presynaptic terminal, activation of a fusion-promoting factor (fpf) and its inactivation, vesicle fusion and depletion, and the general properties of the postsynaptic conductance gates as well as the passive membrane properties of the postsynaptic fiber.

This paper will treat five main topics: (*a*) the relation between the magnitudes of steady-state inward I_{Ca} and that of the EPSP, (*b*) the relationship between the duration of I_{Ca} and that of the EPSP, (*c*) the characterization of the EPSPs after the tail I_{Ca}, (*d*) the differences between the synaptic delay observed at "on" and "off" EPSP, and (*e*) the relation between extracellular calcium concentration ($[Ca^{2+}]_o$) and transmitter release. A model based on the experimental results described here will be presented which reproduces, in general terms, the transmission properties of this synapse during voltage clamp pulses and predicts possible calcium currents and postsynaptic responses following presynaptic action potentials. Phenomena such as facilitation and postsynaptic potentiation will not be considered here.

METHODS

The methodology utilized was similar to that described in the preceding paper (Llinás et al., 1981). In addition to the presynaptic voltage clamp approach described therein, a microelectrode was included which measured the potential of the postsynaptic element in close proximity to the junction.

As in the preceding paper, the sodium conductance (g_{Na}) in the pre- and postsynaptic fibers was blocked by the addition of 5×10^{-6} g/cm^3 tetrodotoxin (TTX) (Narahashi et al., 1964) to the superfusion fluid. The voltage-dependent potassium conductance (g_K) was blocked in both fibers by the addition of 5×10^{-3} M 3- or 4-aminopyridine (3- or 4-AmP) (Pelhate and Pichon, 1974; Llinás et al., 1976; Yeh et al., 1976) to the fluid. The blockage of this conductance in the presynaptic terminal was supplemented by intracellular injection of tetraethylammonium (TEA) (Armstrong and Binstock, 1965).

Evident from reports first made by Bullock (1948) and Bryant (1958) and confirmed by all subsequent studies, oxygenation and the general state of health of the squid are extremely important variables in the maintenance of synaptic transmission. Indeed, in our experience animals demonstrating no bleeding from mantle lacerations or internal damage (incurred during capture) survive in good health for several days in the laboratory holding tanks. Nevertheless, the best synapses (i.e., those which respond to high frequency stimulation without demonstrating irreversible synaptic depletion) were often dissected within 8 h after the squid were captured. The results of our experiments, as a whole, indicated that anoxia or damage to the presynaptic terminal had a more deleterious effect on the release process than on the calcium current itself. Thus, while in most of the experiments reported in the previous paper, calcium current was accompanied by transmitter release, the most variable parameter was the release of transmitter itself, i.e., the steps triggered by the increased $[Ca^{2+}]_i$ were the most fragile. Thus, in the present set of experiments only synapses capable of maintaining consistent levels of transmitter release for several hours were considered. Since both pH and temperature seem to affect the release process, all results reported here were performed at 18°C and at a pH of 7.2. As stated in the accompanying paper, the pH of the medium was kept constant with bicarbonate phosphate or Trizma buffer. Temperature in the recording chamber was monitored with a Bailey thermometer (Bailey Instruments Co., Inc., Saddle Brook, N.J.) and controlled via a Peltier-effect system.

Since most of the findings included in this paper were simultaneously obtained with the calcium current measurements described in the accompanying paper, no further description of techniques will be given here.

RESULTS

Synaptic transmission was characterized, as illustrated in Fig. 1, by a presynaptic action potential which generated, after a synaptic delay of ~1 ms, a postsynaptic spike derived from the postsynaptic potential. The recordings in Fig. 1 were obtained with three microelectrodes in the presynaptic terminal digit (for electrode configuration see Fig. 1 of Llinás et al., 1981) and a single postsynaptic microelectrode 500 μm from the end of the preterminal digit. As is evident in this figure, there was very little difference in the amplitude and duration of the presynaptic action potential recorded at these three points in the preterminal. While the data base for the figures and measurements which follow represent experiments performed over the last 4 yr where close to 100 synapses were successfully clamped (see preceding paper), the results illustrated and measured are only those which showed little variability during the long set of stimuli required for each measurement. The measurements which are included represent, therefore, only a small portion of the total results which corroborate the findings described here but were often incomplete and thus not included here.

Relationship between Presynaptic Voltage Clamp Depolarization and Postsynaptic Response

VOLTAGE CLAMP RESULTS After pharmacological blockage of g_{Na} and g_K, recordings such as those illustrated in Fig. 2 were typically obtained. In this particular case, I_{Ca} was measured by the two-electrode technique (see Llinás et al., 1981). While no threshold was found for the depolarization-release coupling, since I_{Ca} is a continuous function of presynaptic depolarization (cf. Llinás, 1979), in most synapses a 20-mV presynaptic depolarization from a holding potential of -70 mV (i.e., close to the resting potential) was found to be the minimum

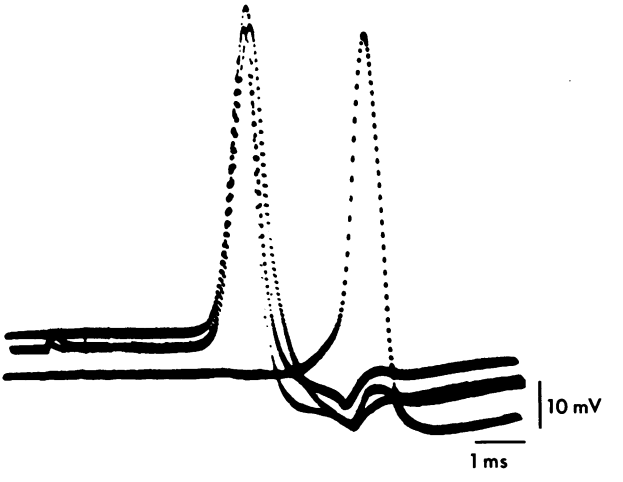

FIGURE 1 Synaptic transmission at the squid giant synapse. Action potentials in the presynaptic terminal simultaneously recorded by three intracellular electrodes. Postsynaptic action potential is seen to develop from a postsynaptic potential. The synaptic delay is close to 1 ms. $[Ca^{2+}]_o$ = 10 mM.

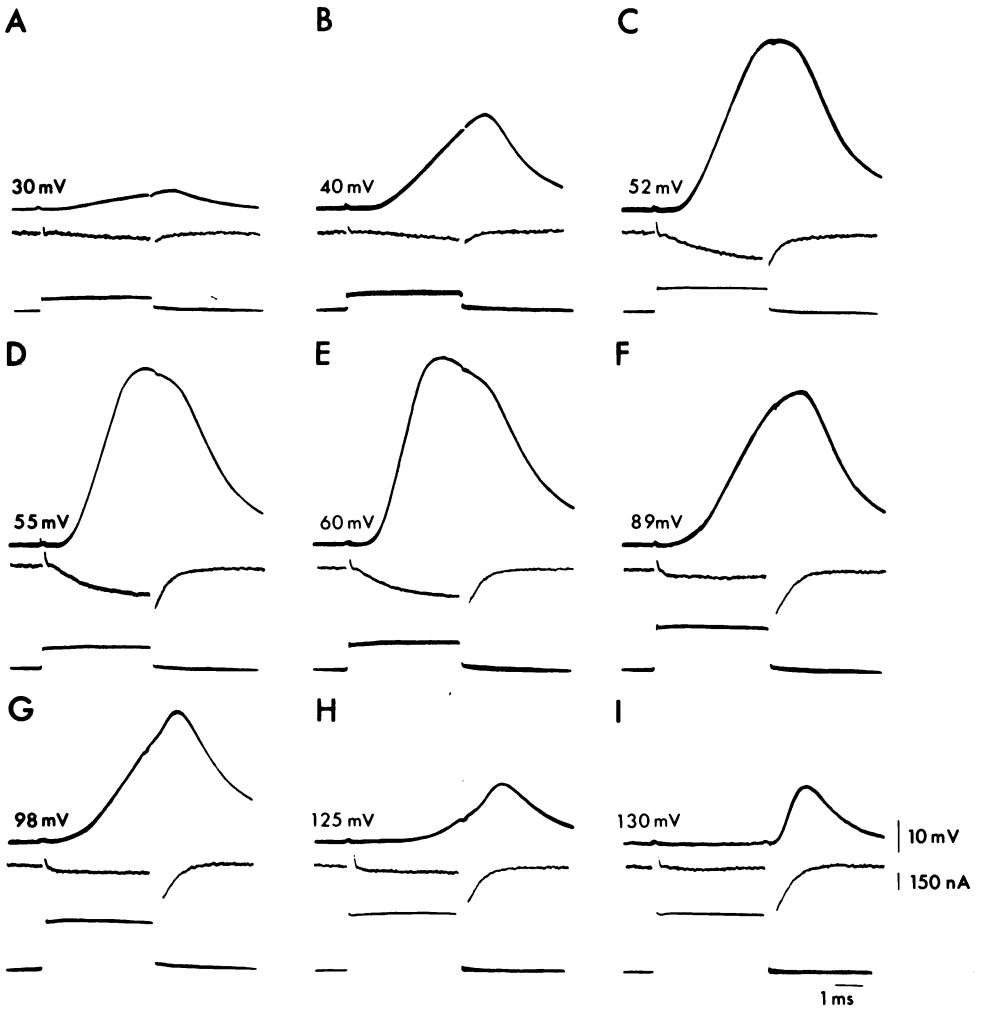

FIGURE 2 Synaptic transmission during voltage clamp of the presynaptic terminal. Top trace, postsynaptic response (EPSP); middle trace, presynaptic calcium current (I_{Ca}); bottom trace, presynaptic voltage pulse (value of presynaptic pulse is given to the left). Maximum presynaptic current, and postsynaptic response occur at 60 mV depolarization. (Sodium and potassium conductances have been blocked with TTX, and TEA/3-AmP, respectively.) $[Ca^{2+}]_o$ = 10 mM.

level for reliable measures of I_{Ca}. Below this level, I_{Ca} was often too close to baseline noise to be properly characterized. Thus, as seen in Fig. 2 *A*, a depolarization of 30 mV from rest produced a small inward current (middle record) which began very slowly and showed a close-to-linear increase with time. At the end of the pulse, a fast tail current was observed. The postsynaptic response generated by this current is seen in the upper record. Note that the EPSP which follows the break of the voltage clamp pulse is associated with the inward tail current. Increasing the amplitude of the presynaptic depolarization step by 10 mV produced a larger EPSP with a faster rate of rise which, as in the previous record, continued to increase

after the termination of the pulse (Fig. 2 *B*). At this level of depolarization the amplitude of I_{Ca} and the EPSP increased in a close-to-linear fashion for the duration of the pulse.

Further increases in presynaptic depolarization (Fig. 2 *C*, *D*, and *E*) produced a change in the shape, rate of rise, and amplitude of the EPSP. At these levels of presynaptic depolarization (52–60 mV) the EPSP reached a peak (*C*) and began to decline (*D*, *E*) during the pulse. The actual rate of rise of the EPSP reached a maximum in most experiments at 60 mV depolarization (*E*) as did the peak of I_{Ca}. In addition, at these levels of depolarization the sigmoidal character of the I_{Ca} onset was evident. However, although there was a clear increase in the I_{Ca} amplitude in *C*, *D*, and *E*, only a small change in the amplitude of the EPSP was observed. This is to be expected from nonlinear summation of the postsynaptic response at high amplitudes (Boyd and Martin, 1956) and from the presence of a certain amount of voltage-dependent g_K in the postsynaptic fiber due to the lack of intracellular TEA injection in this axon.

As the presynaptic voltage increased beyond 60 mV (from *F* to *I*), the rate of rise and amplitude of the "on" EPSP decreased while the "off" response increased. At the same time, the steady-state presynaptic current (as described in the accompanying paper) decreased in amplitude while the tail current amplitude increased to reach a maximum near 110 mV depolarization. In addition, the latency for the onset of the calcium current can be seen to decrease with increases in presynaptic voltage amplitude. Thus, a clear correlation can be seen between the characteristics of presynaptic I_{Ca} and the postsynaptic response. In Fig. 2 *I*, at the suppression potential level, (Katz and Miledi, 1967), no synaptic transmission was observed for the duration of the pulse and a sharp, short-latency, "off" postsynaptic response was generated by the tail current.

Another parameter which varies with levels of presynaptic depolarization is the "on" synaptic delay. This value decreases to a minimum at depolarization of 60–80 mV. With increasing depolarization, the latency again increased, this being especially clear in *H*. As will be discussed later, the differences in shape and synaptic delay of the postsynaptic response are quite important and relate directly to steps preceding transmitter release.

The quantitative relationship between the amplitude of the presynaptic voltage clamp depolarization and the postsynaptic potential is shown in Fig. 3 *A* where the closed circles represent the "on" and the crosses the "off" postsynaptic response. The peak amplitude for the postsynaptic potential occurred near presynaptic depolarization of 60 mV and the suppression potential in the vicinity of 130–140 mV. The amplitude of the "on" EPSP was measured as the maximum level of postsynaptic membrane potential before the termination of the voltage-clamp step. The amplitude of the "off" response was taken as the difference between the "on" EPSP and the maximum postsynaptic potential after the termination of the clamp. Following high levels of "on" transmitter release, the "off" EPSP was smaller than expected, due to partial transmitter depletion. This property, which results in a bimodal plot of Pre *V* vs. "off" EPSP, is also seen in the model (Fig. 3 *A–D*). As shown in Fig. 3 *C*, the rate of rise of the EPSP increased with presynaptic depolarization to reach its maximum value at the same level of presynaptic depolarization as does the EPSP amplitude (Fig. 3 *A* and *B*).

The maximum amplitude of the "off" EPSP (Figs. 2 *I* and 3 *A* and *D*) was quite small compared with that of the "on." This is at variance with results obtained during current clamp (Katz and Miledi, 1967; Kusano et al., 1967; Kusano, 1968; Llinás and Nicholson,

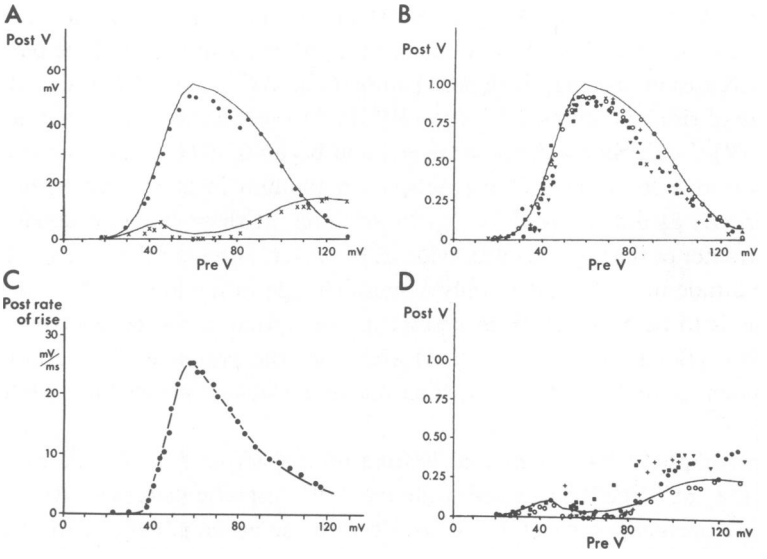

FIGURE 3 Relationship between amplitude of presynaptic voltage clamp step and postsynaptic response. (*A*) Plot of EPSP amplitude against presynaptic voltage for a single synapse. (●), "on" response; (+), "off" response. (*B*) Presynaptic voltage and "on" responses for seven synapses. The EPSP amplitude for each synapse was normalized by setting the maximum response to a value of 1. (*C*) Rate of rise of EPSP as a function of presynaptic voltage. (*D*) Presynaptic voltage and "off" response are plotted for five synapses (amplitudes were normalized by setting maximum "on" response to 1). In *A*, *B*, and *D* solid line is numerical solution for mathematical model of synaptic transmission. $[Ca^{2+}]_o$ = 10 mM.

1975) where the amplitude of the postsynaptic "off" response is similar in size to the "on" potential. This discrepancy is due to the stimulation technique. Thus, under current clamp conditions the presynaptic voltage drop to baseline is very much slower than in the voltage-clamp condition and is often accompanied by a certain amount of self-regenerating calcium entry. Under voltage-clamped conditions, the electronic control of membrane potential prevented such "off" calcium spikes from occurring and thus the amount of transmitter release is determined by the duration and amplitude of the calcium tail current. In Fig. 3 *B* and *D* the "on" and "off" response obtained from several synapses are plotted; here the postsynaptic response has been normalized, the maximum (generally at 60 mV depolarization) corresponding to 1. The continuous line in Fig. 3 *A*, *B*, and *D* represent the numerical solution for Eq. 11. The experimental results match the numerical solution adequately for the "on" response. The match to the "off" response is not as good but falls well within the spread of the data.

RELATIONSHIP BETWEEN CALCIUM CURRENT AND EPSP The relationship between calcium entry and transmitter release is of great interest as it bears directly on the mechanisms responsible for this release. We have found that the dependence of the postsynaptic "on" response on presynaptic voltage resembles quite closely the relationship between presynaptic voltage and the steady-state calcium current (I_{Ca}^{∞}) (Llinás et al., 1976; Fig. 10 in Llinás et al., 1981). However, this relationship is not simple; indeed, the plot of postsynaptic potential as a function of presynaptic I_{Ca} shows hysteresis with increasing levels of presynaptic depolarization. Thus, as I_{Ca} increases (for depolarization up to ~45 mV) a

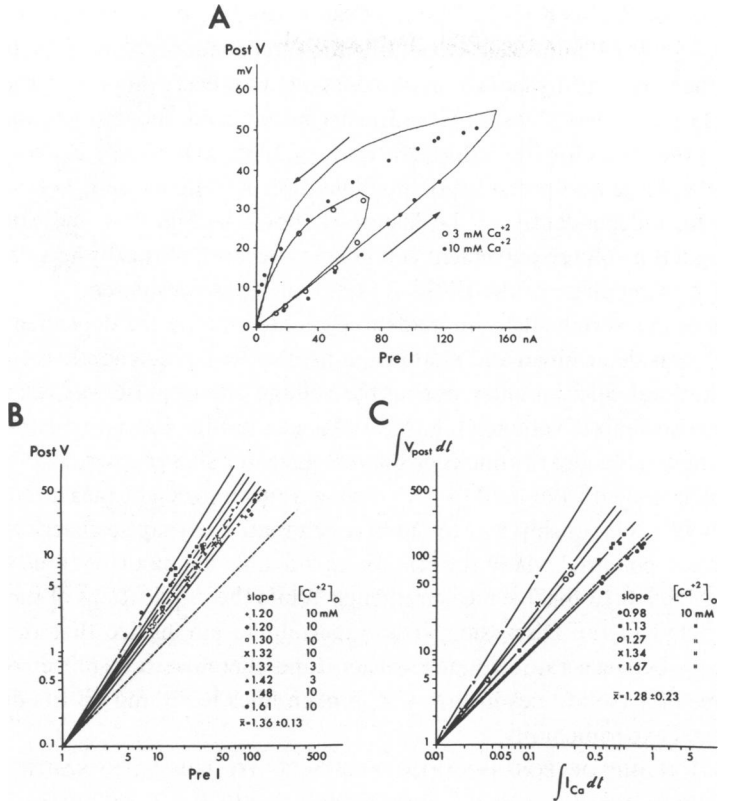

FIGURE 4 Relationship between presynaptic calcium current and postsynaptic response. (*A*) EPSP amplitude is plotted against presynaptic current for two $[Ca^{2+}]_o$. Right-going arrow corresponds to voltage clamp pulses up to 60 mV; left-going arrow to voltage clamp pulses above 60 mV. Solid lines are numerical solutions given by model. (*B*) EPSP amplitude (mV) is plotted against presynaptic current (nA) for five synapses using double logarithmic coordinates. For clarity, presynaptic current for 0.1 mV was set to 1 nA. (*C*) Area under "on" EPSP (V · s) is plotted as a function of total calcium entering the presynaptic terminal (nC). Presynaptic charge displacement for 1 V · s postsynaptic response was set to 0.001 nC. In *B* and *C*, only EPSPs after presynaptic depolarizations <60 mV were plotted. $[Ca^{2+}]_o$ = 10 mM unless indicated. Dashed lines in *B* and *C* are values given by the mathematical model. Note double logarithmic coordinates in *B* and *C*.

linear relationship is seen between this current and the amplitude of the EPSP (Fig. 4 *A*, right-going arrow). However, as I_{Ca} and the EPSP amplitude approach their maximum values, the slope of the relationship increases (Fig. 4 *A*). Then, as the I_{Ca} and EPSP amplitude decrease (for presynaptic depolarization above 60 mV), hysteresis is observed in the I_{Ca}-EPSP relationship (left-going arrow, Fig. 4 *A*). Although this hysteresis may be due in part to the greater total entry of calcium at higher levels of presynaptic depolarization (due to the faster onset of I_{Ca}), this cannot account entirely for the observation as some hysteresis (although less) is seen in the plot of $\int V_{post}\, dt$ versus $\int I_{Ca}\, dt$. Further, the hysteresis does not seem to be related to the magnitude of $[Ca^{2+}]_o$ as it is also seen in 3 mM as well as in 10 mM calcium (Fig. 4 *A*). As will be discussed later when describing the results from the model, the hysteresis most likely reflects a voltage dependence for the calcium-release coupling. This

dependence can also be seen if the ratio, $\int \text{Post } V\, dt / \int I_{Ca}\, dt$, is plotted as a function of presynaptic voltage. If calcium release coupling were to be independent of the transmembrane electric field, then this ratio should remain constant. However, this is not the case. For the data shown in Fig. 2, if the values for this ratio are normalized, they range from 1 (89 mV) to 0.11 (125 mV); the mean for five values (ratios for 52, 55, and 60 mV cannot be included as the "on" EPSP is large and postsynaptic nonlinearities are introduced) is 0.53 with a SD of 0.40. These data, independently of the histeresis shown in Fig. 4 *A*, indicate that calcium release coupling has a voltage-dependent component. Because of this hysteresis, in subsequent analysis only the rising phase of the EPSP-I_{Ca} relationship is considered.

Two classes of measurements were made to evaluate directly the dependence of the EPSP on I_{Ca}^{∞}. First, I_{Ca}^{∞} was determined and plotted against the peak postsynaptic response (Fig. 4 *B*) and, second, the total calcium entry during the voltage-clamp pulse was related to the time integral of the postsynaptic voltage (Fig. 4 *C*). As seen in Fig. 4 *B*, postsynaptic peak plotted against I_{Ca}^{∞} (using double logarithmic coordinates) gave, for six synapses, a set of straight lines with slopes which ranged from 1.20 to 1.61 having a mean for eight measurements of 1.36 ± 0.13. A very similar relationship was found between total presynaptic charge and the integral of the postsynaptic potential where the relation in a double log plot (for three synapses) has a mean slope of 1.28 ± 0.23 for five measurements. While the implications of these findings will be treated in detail in the Discussion, it is important to emphasize that the model, which assumes linearity between rate of vesicle fusion (and therefore transmitter release) and I_{Ca} and thus a slope of 1 (solid lines in Fig. 4 *A*, broken lines for *B* and *C*) fits quite closely the slopes determined experimentally.

RELATIONSHIP OF POSTSYNAPTIC RESPONSE TO THE PRESYNAPTIC CLAMP PULSE DURATION Voltage-clamp pulses of increasing duration (0.4–4.7 ms) but constant amplitude (40 mV) produced postsynaptic responses characterized by a constant rate of rise for pulses >1.5 ms (Fig. 5 *A*). For clamp pulses <1.5 ms, the postsynaptic potential is mainly an "off" EPSP which, for low amplitudes of presynaptic voltage steps, has a slower rate of rise than the

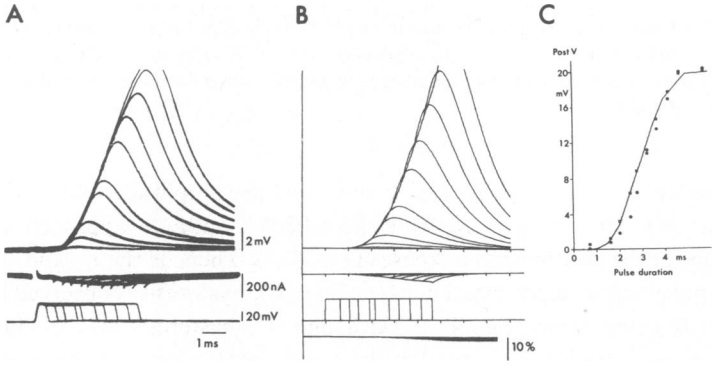

FIGURE 5 Effect of duration of presynaptic voltage step on synaptic transmission. (*A*) Experimental results. Top trace, postsynaptic response; middle trace, calcium current; bottom trace: presynaptic voltage pulse. (*B*) Mathematical model. Top trace, postsynaptic response; second trace, presynaptic calcium current; third trace, presynaptic voltage pulse; bottom trace, vesicle depletion (expressed as percent of immediately available store). (*C*) Plot of postsynaptic response amplitude as a function of pulse duration for two synapses. Solid line given by mathematical model. $[Ca^{2+}]_o$ = 10 mM.

"on" EPSP. The comparison of these responses with those obtained by the computer model (Eq. 11), illustrated in Fig. 5 *B*, indicates a good match for the rate of rise and overall time course between the experimental results and the model. In addition, the model can determine (based on Eq. 6) the degree of transmitter depletion occurring for these voltage-step duration (Fig. 5 *B*, bottom trace; and see below). A plot of prepulse duration against EPSP amplitude is given in Fig. 5 *C*. Agreement between the experimental data (solid circles and squares) and the computer model (solid line) once again supports the suggestion of a linear relationship between these two variables. Similar types of EPSPs with a close to constant rate of rise during a prolonged stimulus have been recently described in the crab (Blight and Llinás, 1980) and in Aplysia (Shapiro et al., 1980).

Transmitter Depletion

An added complexity of the functional properties of this synapse is the phasic nature of its transmitter release. In contrast to synapses that are tonic in function, e.g., retinal neurons (Dowling, 1970), it is well known that the squid giant synapse is incapable of maintaining a high level of release for a protracted period (Kusano and Landau, 1975). Thus, the amplitude and time course of the postsynaptic response to prolonged presynaptic depolarizations were examined. (In these experiments, relatively low levels of presynaptic depolarization were used to eliminate the decrease in potential due to postsynaptic nonlinearities.) As shown in Fig. 6 *A*, a decrease in the amplitude of the postsynaptic response is seen for a 40-ms voltage-clamp pulse. Note that this prolonged depolarization generated a postsynaptic response which dropped by 50% of its initial amplitude in 34 ms and was accompanied by a small "off" response. The time course for this decrease was found to be very much in agreement with similar findings by Katz and Miledi (1969, 1971) and by Kusano (1968). Obviously, the decrease in amplitude of the postsynaptic response can be ascribed, in addition to transmitter depletion, to other parameters such as inactivation of the calcium channel (Baker et al., 1971) and postsynaptic receptor desensitization (cf. Neher and Stevens, 1976). However, the

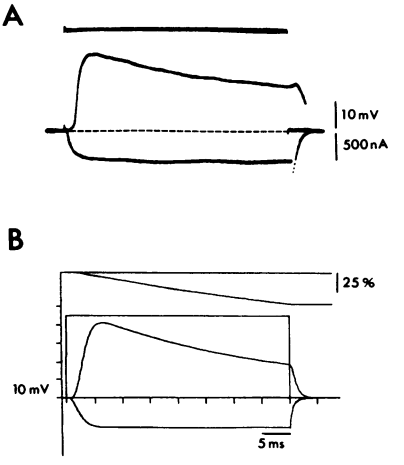

FIGURE 6 Prolonged voltage clamp pulse. (*A*) Experimental results. Top trace, presynaptic voltage; middle trace, postsynaptic response; bottom trace, presynaptic current. (*B*) Mathematical model. Top trace, vesicle depletion (expressed as percent of immediately available store). $[Ca^{2+}]_o$ = 40 mM.

protracted transmission obtained at low voltages and the absence of any change in the current trace suggests that for these durations (up to 100 ms) calcium inactivation or receptor desensitization are rather unlikely.

The possibility that this reduction was produced by transmitter depletion was indirectly tested by the introduction of a depletion parameter into the model (Fig. 6 *B*, first trace) and, as will be seen later, given reasonable assumptions regarding the mechanism for this depletion, when this factor is included the model is capable of closely reproducing the complicated waveforms obtained for different presynaptic voltages and duration. Moreover, this assumed depletion becomes an important parameter in the proper simulation by the model, of the complex shape of the EPSP during voltage clamp.

Tail Calcium Current and "Off" EPSP; the Question of Synaptic Delay

Among the most significant points in characterizing the relation between tail I_{Ca} and the EPSP relates to the fact that during the tail I_{Ca} an instantaneous calcium inflow occurs which allows the study of the transmission process independently of the "on" calcium kinetics. Two aspects of synaptic transmission were considered in studying the relation between tail currents and the "off" EPSP. The first concerns the relationship between the amplitude of the tail current and that of the "off" response (Fig. 7). Indeed, as plotted in Fig. 7, and as expected from our previous measurements, the relation of the two was found to be close to linear giving slopes of 0.75–1.34 mV (mean 1.11 ± 0.22; n = 4) when plotted on double log coordinates. The broken line in Fig. 7 is the relationship obtained from our model (slope 0.81). A second interesting feature related to the minimum synaptic delay encountered for the "on" and "off" EPSPs (Fig. 8). The delay for the "on" response is taken as the time between the onset of the voltage clamp pulse and that for the postsynaptic voltage. The "off" delay is measured using a voltage clamp pulse at or above the suppression potential. The interval between the "break" of the voltage clamp pulse and the beginning of the "off" response is the delay. Thus, for a 60-mV square pulse depolarization, a delay of 733 μs was observed for the "on" response (Fig.

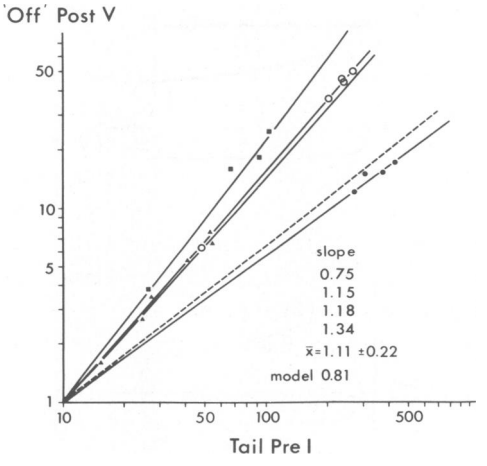

FIGURE 7 Relationship between amplitude of presynaptic tail current and "off" EPSP amplitude. Results for four synapses are shown. The mean increase in EPSP amplitude per decade increase in current is 1.11 (± 0.22). Tail current for 1 mV EPSP was set to 10 (arbitrary units). $[Ca^{2+}]_o$ = 10 mM.

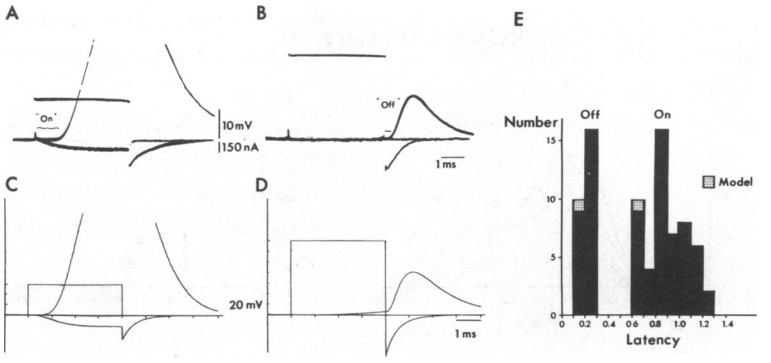

FIGURE 8 Synaptic delay for the "on" and "off" EPSP. The "on" response is shown for a 60-mV presynaptic voltage clamp; 733 μs latency. (*B*) The "off" response is seen following a voltage clamp to the suppression potential (140 mV); 200 μs latency. (*C* and *D*) EPSPs generated by the mathematical model for a 60-mV clamp ("on" response latency, 675 μs), and a 140-mV clamp ("off" response latency, 150 μs). (*E*) Histogram showing the variation in latency observed for the "on" response (mean 0.894 ± 0.168, n = 51), and the "off" response (mean 0.192 ± 0.27, n = 25). "On" delay was determined near the maximum EPSP amplitude, "off" delay at the supression potential.

8 *A*). On the other hand, the delay for the "off" response in the same synapse (Fig. 8 *B*) was much shorter (200 μs). The model (Fig. 8 *C* and *D*) gives values of 675 and 150 μs for the same values of presynaptic depolarization. A histogram of the "on" and "off" delays is shown in Fig. 8 *E* and indicates that the "on" delay fluctuated between 0.633 and 1.27 ms with a mean of 0.894 ± 0.17 ms (n = 51) and the "off" delay between 133 and 233 μs with a mean of 192 ± 27 μs (n = 25). Thus, the synaptic delay may be viewed as having two components, *a* and *b* (Llinás, 1977), the first representing the time dependence for the onset of the calcium current and the second the time dependence of the subsequent steps leading to the postsynaptic potential (see insert, Fig. 13 *A*).

The two components show different voltage dependences. The *a* component depends on the calcium channel kinetics and the *b* component depends on the kinetics of the calcium release coupling. The *a* delay decreases with presynaptic voltage. The *b* component has a more complex relation with respect to both I_{Ca} and the size of the transmembrane field. A detailed study of the voltage and I_{Ca} dependence of synaptic delay is presently in progress.

Of the different measurements made, this is indeed one of the most significant since it sets time limits to the possible processes involved in transmitter release and for the distance between the site of I_{Ca} entry and that of the secretory event. As stated above, the difference between the "on" and "off" delays relates to the onset of the calcium conductance and, more important, the short delay for the "off" response suggests that the site of calcium entry must be located quite near the release site. These points, as well as a comparison with the delays obtained by the model (Fig. 8 *C* and *D*), will be treated in the Discussion.

Relationship between Extracellular Calcium Concentration and Postsynaptic Potential

Modification of the $[Ca^{2+}]_o$ has proven a useful technique in describing the calcium dependence of synaptic transmission (cf. Blaustein et al., 1978 *a*; Rahamimoff et al. 1978). For this reason, a set of studies was undertaken to determine the relationship between calcium

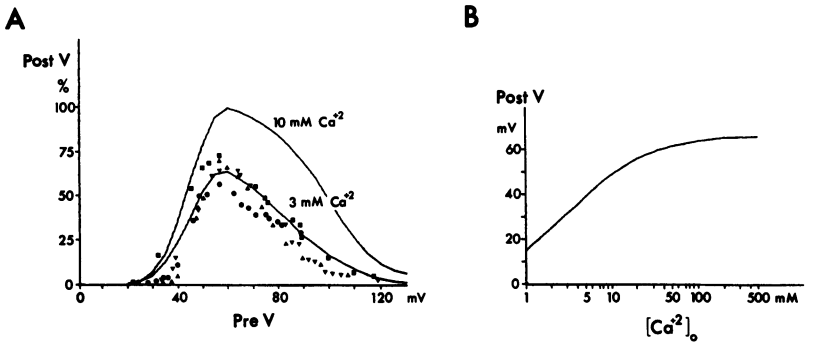

FIGURE 9 Extracellular calcium concentration and postsynaptic response. (*A*) Results of mathematical model (solid lines) are shown for 3, and 10 mM $[Ca^{2+}]_o$. Data for 3 mM $[Ca^{2+}]_o$ is shown in four synapses (see Fig. 3 *B* for data for 10 mM $[Ca^{2+}]_o$). (*B*) Amplitude of EPSP generated by the mathematical model for a 60-mV presynaptic pulse in various $[Ca^{2+}]_o$ is plotted against $[Ca^{2+}]_o$ on semilogarithmic coordinates.

concentration and transmitter release utilizing voltage clamp. The maximum EPSP obtained in 10 mM calcium for each synapse was set to 100% and EPSP amplitudes obtained for each synapse in 3 mM calcium are expressed relative to this value. In Fig. 9 *A*, the values obtained by our model at 3 and 10 mM calcium are given by solid lines; for clarity, experimental points are given only for 3 mM calcium (see Fig. 3 *B* for fit of data to model at 10 mM calcium). As illustrated in Figs. 9 *A* and 4 *A* the relationship between presynaptic potential and transmitter release is dependent on the amount of extracellular calcium. Furthermore, the relationship between $[Ca^{2+}]_o$ and suppression potential and that between $[Ca^{2+}]_o$ and peak response are seen to be clearly calcium-dependent. Comparison of experimental results in Fig. 9 *A* with those obtained from the computer model (solid lines) indicate that the assumption regarding the dependency of postsynaptic response on $[Ca^{2+}]_o$ proposed in the model (see below) is justified. The "on" postsynaptic potential amplitude as a function of $[Ca^{2+}]_o$ for 60 mV presynaptic depolarization, as determined by Eq. 11 of our model, is plotted in Fig. 9 *B* using semilogarithmic coordinates and indicates that above 1 mM calcium there is an exponential relationship between $[Ca^{2+}]_o$ and transmitter release. The postsynaptic response (and I_{Ca}) begins to saturate at ~10 mM $[Ca^{2+}]_o$. A list of results obtained from several synapses at different calcium concentrations is given in Table I. While sets of results for $[Ca^{2+}]_o$ ranging from 3 to 100 mM were obtained in these studies, a systematic effort was concentrated on the difference between 3 and 10 mM $[Ca^{2+}]_o$ as it seemed the more significant range. A more detailed study of $[Ca^{2+}]_o$ and the effects of other divalent cations on synaptic transmission is now in progress.

Mathematical Model for Description of Relationship between Presynaptic Currents and Postsynaptic Responses

Several factors must be considered when modeling the relation between the voltage-dependent entry of calcium current and the postsynaptic responses triggered by such current. The high specificity of calcium ions in promoting vesicle fusion and transmission release (cf. Katz, 1969) strongly suggests that a specific binding entity for calcium, probably a protein, is involved in the process (Parsegian, 1977; Baker and Schaepfer, 1978). Upon binding calcium,

TABLE I
PEAK POSTSYNAPTIC VOLTAGE (PV) AND PRESYNAPTIC CURRENT (I_{Ca}) AT VARIOUS $[Ca^{2+}]_o$

Synapse No.	$[Ca^{2+}]_o$	Peak PV	I_{Ca} at peak PV	Slope PV vs. I_{Ca}	Slope $\int PV\,dt$ vs. $\int I_{Ca}\,dt$
	(mM)	*(mV)*	*(nA)*		
S714-0	3	19	79	—	—
S714-3	3	28	168	1.32	—
S818-2	3	28	175	—	—
S819	3	7	150	—	—
S823	3	30	65	1.42	—
Mean ± SD		22.3 ± 8.8	127 ± 46		
S273	10	14	550	—	—
S274	10	14	400	1.3	1.27
S714-0	10	35	210	1.48	—
S714-2	10	50	140	1.2	—
S714-3	10	48	320	1.2	—
S714-4	10	15	125	1.61	—
S717-1	10	64	216	—	—
D717-2	10	65	236	—	—
S719	10	50	200	—	0.98
S725	10	44	392	—	1.67
S725	10	48	440	—	1.34
S725	10	32	400	—	1.13
S818	10	36	370	—	—
S827	10	53	289	—	—
S874	10	51	250	1.32	—
S875	10	53	289	—	—
S878	10	48	250	1.2	—
Mean ± SD		41.9 ± 16.3	298.6 ± 110		
S691	20	30	225	—	—
S692	20	63	379	—	—
S693	20	65	360	—	—
S714-0	20	64	526	—	—
Mean ± SD		55 ± 14.6	373 ± 107		
S714-0	100	70	840	—	—

this entity presumably undergoes a conformational change and catalyzes the fusion between synaptic vesicles and the plasma membrane. Such a factor is included in this model and will be referred to as the fusion-promoting factor (fpf). The equilibrium and kinetics contants characterizing the above processes will, of course, affect the course of transmitter release and, ultimately, the postsynaptic response. We must further assume that as fusion is initiated, vesicles are depleted from the immediate vicinity of the plasma membrane (the immediately available store) and that this may become a factor in the transmission process.

Other parameters to be considered relate to the opening and closing time constants of the gating of the postsynaptic receptor-transmitter complex and the electrical time constant of the postsynaptic terminal membrane. Since in these experiments postsynaptic voltage rather than current has been recorded, the relation between the two was accounted for in the computations, thus obviating the need for an explicit correction of the type suggested by Boyd and Martin (1956). Finally, the time required for the diffusion of the transmitter across the

synaptic gap is expected to be very short (~1 μs for a gap width of 200 Å and a diffusion coefficient of 10^{-6} cm^2/s) and thus is not a significant consideration for the time scales under discussion.

It is clear then that many steps and rate constants intervene between the flow of calcium ions into the presynaptic terminal and the subsequent postsynaptic voltage change. Because of the inherent complexity of such a sequence, and since the parameters themselves may interact in a negative or positive manner, such steps may not be individually correlated to I_{Ca} or EPSP amplitude. Thus, this model was attempted in order to formulate a plausible picture of the process of synaptic transmitter release including a set of reasonable intermediate steps. Sets of values for the parameters controlling each step were chosen such that the model fit reasonably the data available. Of course, these values, and indeed the assumptions underlying the model, are not unique but together form one possible model of chemical synaptic transmission.

Presynaptic Steps

ACTIVATION OF THE FUSION-PROMOTING FACTOR The behavior of fpf is assumed to be as follows. If a pulse of calcium ions enters the presynaptic digit, fpf binds these ions, forming a complex (fpf · Ca^{2+}) in proportion to $[Ca^{2+}]_i$ and the time of exposure to the calcium ions. This complex then becomes activated by first-order kinetics into a species fpf* · Ca^{2+} which facilitates fusion of vesicles with the plasma membrane at a rate in proportion to its amount. The species fpf* · Ca^{2+} can then revert into a nonactive form, again by a first-order kinetics. Similarly, the complex fpf · Ca^{2+} can be inactivated directly without being converted first into fpf* · Ca^{2+}. The chain of events may thus be summarized as follows:

$$\begin{array}{l} \text{fpf} \cdot Ca^{2+} \xrightarrow{k_a} \text{fpf*} \cdot \text{Ca}^{2+} \xrightarrow{k_i} \text{inactive form} \\ \downarrow\ k_b \\ \text{inactive form,} \end{array}$$

where k_a is the rate constant for activation and k_b and k_i are the rate constants for the inactivation of fpf · Ca^{2+} and fpf* · Ca^{2+}, respectively. The values for these constants were chosen in order to obtain a best fit to the data for a 60-mV depolarization. After this, values were determined to obtain a fit to the data for eleven other levels of depolarization. These values were plotted against presynaptic depolarization and a line connecting the points drawn by hand (Fig. 10). Rate constants for additional voltage-clamp levels were chosen such as they fell on the line. In this way, rate constants for 23 levels of depolarization were chosen and stored in a table for the model-generated EPSPs (Fig. 12).

In response to a brief impulse of calcium, the following expressions are obtained for [fpf · Ca^{2+}]:

$$\frac{d[\text{fpf} \cdot \text{Ca}^{2+}]}{dt} = k[\text{fpf}] \cdot [\text{Ca}^{2+}]_i - (k_a + k_b)[\text{fpf} \cdot \text{Ca}^{2+}], \quad (1)$$

where k is a proportionality constant and

$$\frac{d[\text{fpf*} \cdot \text{Ca}^{2+}]}{dt} = k_a[\text{fpf} \cdot \text{Ca}^{2+}] - k_i[\text{fpf*} \cdot \text{Ca}^{2+}], \quad (2)$$

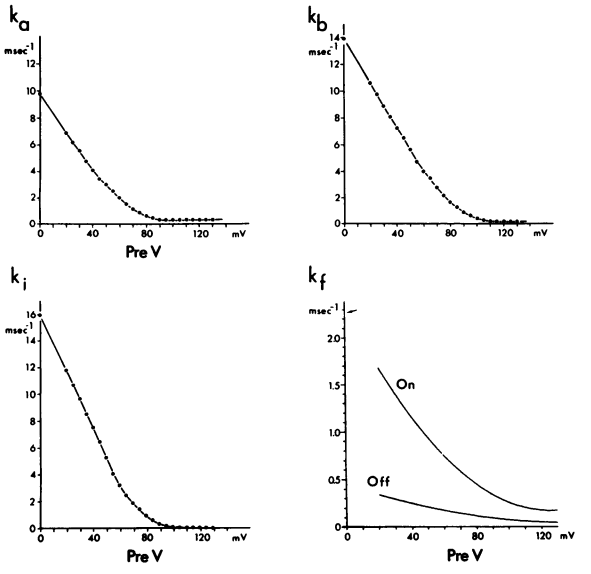

FIGURE 10 Voltage dependence of presynaptic rate constants. During the "on" release k_a, k_b, and k_i assume values determined by the field across the presynaptic membrane; these values are plotted here. At the end of the voltage clamp pulse, these rate constants assume the value appropriate to 0 mV depolarization (y intercept). k_f, the rate constant for vesicle fusion, is voltage-dependent during "off" release as well as "on" release for voltage clamp pulses (arbitrary scale). For action potentials, however, k_f assumes the value appropriate for "on" release at 0 mV depolarization (the y intercept for "on" release, arrow).

which yields the following expression for [fpf* · Ca^{2+}]:

$$[\text{fpf}^* \cdot Ca^{2+}] = \frac{Ak_a}{k_i - (k_a + k_b)} [\exp^{-(k_a+k_b)t} - \exp^{-k_i t}], \tag{3}$$

where A is a constant which depends on the magnitude of the $[Ca^{2+}]_i$ pulse.

Since $[Ca^{2+}]_i$ cannot be determined directly, it is necessary to correlate the calcium concentration at the plasma membrane with the calcium current flowing into the presynaptic digit (see preceding paper). Calcium ions flowing into the cell through a channel are assumed to diffuse radially and, thus, for a constant ion influx a steady state is rapidly reached (cf. Parsegian, 1977). The time required to reach one-half the steady-state value is estimated to be ~35 μs even assuming a low diffusion coefficient for calcium of 10^{-6} cm^2/s and a hemisphere of 750 Å radius for the active zone (Pumplin and Reese, 1978).

The time course for the build-up of $[Ca^{2+}]_i$ upon influx of calcium ions through a cluster of channels may be estimated theoretically. In fact, the solution to a similar problem relating to the conduction of heat in solids has been presented by Carslaw and Jaeger (1959). Modifying their notation to the one used in this paper, the $[Ca^{2+}]_i$ at time t, for a constant flux, J, is given by:

$$[Ca^{2+}]_i = \frac{Jr_0^2}{Dr}\left\{\text{erfc}\frac{r - r_0}{2(Dt)^{1/2}} - \exp\left[\frac{r - r_0}{r_0} + \frac{Dt}{r_0^2}\right]\text{erfc}\left[\frac{r - r_0}{2(Dt)^{1/2}} + \left(\frac{Dt}{r_0^2}\right)^{1/2}\right]\right\} \tag{4}$$

where r_o is the radius of the hemisphere, r is the radial distance from the origin, erf$c$ stands for the complement error function, and D is the diffusion constant for Ca^{2+} in the cytoplasm.

For $[Ca^{2+}]_i$ at the site of influx, we substitute $r = r_o$, i.e.,

$$[Ca^{2+}]_i = \frac{Jr_0}{D}\left[1 - \exp\frac{Dt}{r_0^2}\,\mathrm{erf}c\left(\frac{Dt}{r_0^2}\right)^{1/2}\right]. \tag{5}$$

The asymptotic value that $[Ca^{2+}]_i$ reaches after a long time is Jr_o/D, and the time course to reach this value is given by the expression in the last bracket. Using Appendix II of Carslaw and Jaeger, we can estimate that it takes ~35 μs to reach 50% of the asymptotic value for r_o = 750 Å and $D = 10^{-6}$ cm^2/s, assuming a hemipherical rather than disklike channel cluster. This latter assumption is not expected to change significantly the estimated time to steady-state conditions. The value for r_o was chosen such that the surface area of the hemisphere was equal to that of a single active zone in the squid presynaptic terminal (Pumplin and Reese, 1978). (Since these active zones are disk shaped, an r_o = 750 Å for a hemisphere is equivalent to a disk with a 1,500 Å radius.)

The distribution of calcium within the terminal as given by the numerical solution Eqs. 4 and 5 are shown in Fig. 11. The increase in $[Ca^{2+}]_i$ at the membrane surface for various levels of I_{Ca} is given in Fig. 11 *A*. Note that the asymptotic value is reached by ~200 μs. The value for $[Ca^{2+}]_i$ at 200 μs at varying distances from the membrane is shown in Fig. 11 *B* for a single level of I_{Ca} (200 nA). Note that $[Ca^{2+}]_i$ falls to one-half its value at ~390 Å. This same relationship is expressed in Fig. 11 *C* where the time course of increase in $[Ca^{2+}]_i$ at varying distances from the surface is given for a current flow of 200 nA. Finally, in Fig. 11 *D* the value for $[Ca^{2+}]_i$ as a function of distance is shown for several times following the onset of a 200-nA current.

It must be emphasized that the actual values for $[Ca^{2+}]_i$ cannot be determined at this time and that those in Fig. 11 are maximum values. There are two reasons for this assertion: (*a*) The diffusion constant for calcium in the presynaptic terminal is not known; the value of 10^{-6} cm^2/s was derived from measurements by Hodgkin and Keynes (1957) and Baker (1972) on squid postsynaptic axoplasm. (*b*) Uptake, buffering, or sequestering of calcium within the terminal (Blaustein et al., 1978 *b* and *c*) was not taken into account directly. The low diffusion constant very likely results in part from binding of calcium; however, there is most probably additional calcium buffering. (This is considered indirectly in the model by the pathway whereby the fpf · Ca^{2+} is inactivated directly.) Note that the time course for $[Ca^{2+}]_i$ is independent of its magnitude. Fig. 11 does tell, however, that the time course for increase in $[Ca^{2+}]_i$ is fast and that it falls off rapidly with distance, reaching one-half its value at the limits of the first layer of vesicles. From these calculations it seems evident that the calcium ion concentration at the plasma membrane will follow closely in time the profile of the calcium current and, for events taking place in the millisecond time scale, $[Ca^{2+}]_i$ may be taken to be proportional to I_{Ca}.

An alternative model which will yield an identical mathematical expression for [fpf* · Ca^{2+}] is as follows. Suppose that a constant fraction of the calcium ions entering the presynapse binds to fpf to form fpf · Ca^{2+} (the rest diffusing rapidly away or being removed by calcium-binding proteins present in the presynaptic terminal [Alema et al., 1973; Baker, 1972; Blaustein et al., 1978 *c*]). The entity fpf is assumed to be in excess with respect to the

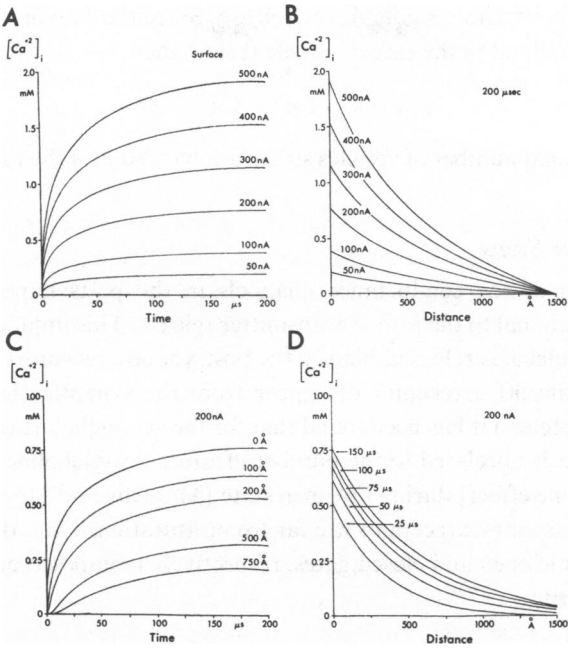

FIGURE 11 Distribution of $[Ca^{2+}]_i$ as determined by Eqs. 4 and 5. A constant flux of calcium is assumed to flow radially into the cytoplasm through a hemisphere of 750 Å radius. (*A*) $[Ca^{2+}]_i$ at the surface of the hemisphere as a function of time for various calcium currents. (*B*) Distribution of $[Ca^{2+}]_i$ within the presynaptic terminal 200 μs after the beginning of a constant flux of calcium of various amplitudes. (*C*) Change in $[Ca^{2+}]_i$ with time at various distances within the presynaptic terminal for a 200-nA current. (*D*) Distribution of $[Ca^{2+}]_i$ within the presynaptic terminal at various times after the onset of a 200-nA calcium current. $D = 10^{-6}$ cm^2/s.

calcium and is not saturated. Assume next that fpf · Ca^{2+} either splits into its constituents with a rate constant k_b or is transformed into fpf* · Ca^{2+} with a rate constant k_a. The fpf* · Ca^{2+} is then inactivated with a rate constant k_i by splitting into its constituents. Last, assume that calcium which splits off either fpf · Ca^{2+} or fpf* · Ca^{2+} is no longer available to fpf because it diffuses rapidly away or is bound to background proteins. The scheme can thus be represented by:

$$\text{fpf} + Ca^{2+} \xrightarrow[\text{step}]{\text{fast}} \text{fpf} \cdot Ca^{2+} \xrightarrow{k_a} \text{fpf}^* \cdot Ca^{2+} \xrightarrow{k_i} \text{fpf} + Ca^{2+}$$
$$\downarrow k_b$$
$$\text{fpf} + Ca^{2+}$$

which will yield Eq. 3 for [fpf* · Ca^{2+}]. It may be noted that in this model the relation between $[Ca^{2+}]_i$ and I_{Ca} is immaterial since it is assumed that a fixed fraction of Ca^{2+} which enters the presynapse binds to fpf, and this is determined directly by I_{Ca}.

RATE OF FUSION OF VESICLES The rate of transmitter release obviously depends on the number of vesicles available at the plasma membrane at the moment under consideration. Again, this was taken to be governed by first-order kinetics and thus, other things being equal, the rate of transmitter release decreases in proportion to the decrease, due to fusion, in the

number of vesicles immediately available for release. Since the rate of transmitter release J_{TR} is obviously directly related to the rate of vesicle fusion, then

$$J_{TR} = k_f \cdot \text{fpf}^* \cdot Ca^{2+} \cdot Q, \tag{6}$$

where Q is the fractional number of vesicles still available and k_f is the rate constant for vesicle fusion.

Postsynaptic Steps

The rate of opening of the conductance channels in the postsynaptic terminal has been assumed to be proportional to the rate of transmitter release. This implies that a fixed fraction of the transmitter molecules released bind to the postsynaptic receptors, and that transmitter molecules which come off a receptor disappear from the synaptic cleft and are no longer available to the receptors. (It has been found that for the acetylcholine receptor the kinetics of the postsynaptic gate is unrelated to the number of times acetylcholine binds to the receptor [i.e., it is an all-or-none effect] during the open state [Magleby and Stevens, 1972].) It is also assumed that the postsynaptic receptors are far from saturation. Thus, denoting by G•TR and G*•TR the postynaptic open and closed gates, respectively (composed of transmitter-receptor complex), one can write:

$$G \cdot TR \xrightarrow{k_g} G^* \cdot TR \xrightarrow{k_{-g}} G + TR. \tag{7}$$

Hence,

$$\frac{d[G \cdot TR]}{dt} = -k_g[G \cdot TR], \tag{8}$$

and

$$\frac{d[G^* \cdot TR]}{dt} = k_g[G \cdot TR] - k_{-g}[G^* \cdot TR]. \tag{9}$$

k_g and k_{-g} are the rate constants for opening and closing (k_g = 20 ms^{-1}; k_{-g} = 4 ms^{-1}) respectively, of the postsynaptic conductivity channels which respond to the transmitter. The conductivity response (I_{EPSP}) to an impulse of transmitter is given by:

$$I_{EPSP} = \text{constant } [G^* \cdot TR] = \text{constant } \frac{k_g}{k_g - k_{-g}} [\exp(-k_{-g}t) - \exp(-k_g t)]. \tag{10}$$

The postsynaptic potential, V, is thus obtained by integrating the following equation:

$$\frac{dV}{dt} = P_3(E_{EPSP} - V) \int_0^t J_{TR}(t - \tau) I_{EPSP}(\tau) d\tau - P_4 V, \tag{11}$$

where E_{EPSP} is the equilibrium potential for the EPSP (+20 mV; Llinás et al., 1974), P_3 and P_4 are proportionality factors, P_3 (35,000) incorporates Martin's correction and is proportional to the reciprocal of the membrane capacitance, and P_4 (0.8) is the reciprocal electrical time constant of the postsynaptic terminal.

Blockage of the voltage-dependent postsynaptic potassium conductance by 3-AmP is both

time- and voltage-dependent (Pelhate and Pichon, 1974; Yeh et al., 1976; Llinás et al., 1976). Thus, the postsynaptic g_K resulting from this incomplete blockage was taken into consideration in the computation of the postsynaptic voltage. As the time and voltage dependence of the drug action has been shown to be linear, and to have a threshold (Yeh et al., 1976; Meves and Pichon, 1977), a potassium current with these characteristics was assumed to exist in the postsynaptic membrane [$I_K = (P_5V_m)(P_6t)$, where t is the time following the onset of I_K]. The threshold voltage (25 mV) and the constants P_5 (1.4) and P_6 (10^{-5}) were chosen to fit the postsynaptic potential generated by a 60-mV, 4 ms, voltage clamp pulse in 10 mM calcium. The current was substracted from the transmitter-dependent postsynaptic current. This treatment of the effect of incomplete blockage by 3-AmP was possible since the postsynaptic current and potential were evaluated simultaneously in the computer execution of the model.

The computations of EPSP amplitude and time course from the above model were compared to postsynaptic responses similar to those described in Fig. 2. The parameters were initially adjusted to attain a best fit as explained above (Fig. 10). The results are shown in Fig. 12, and the values of the pertinent parameters given in Fig. 10. Only relative values at various voltages can be assigned to k_f since the determination of its absolute value requires knowledge of the absolute magnitude of $[Ca^{2+}]_i$. The value of k_f was adjusted to yield ~8% depletion at 60 mV for the 4-ms clamp based on measurements of the decay in the postsynaptic response with long clamps (100 ms). At other selected depolarizations, k_f was chosen to fit the experimental data. A least squares fit was obtained for these (nine) points and the values thus determined were used for k_f.

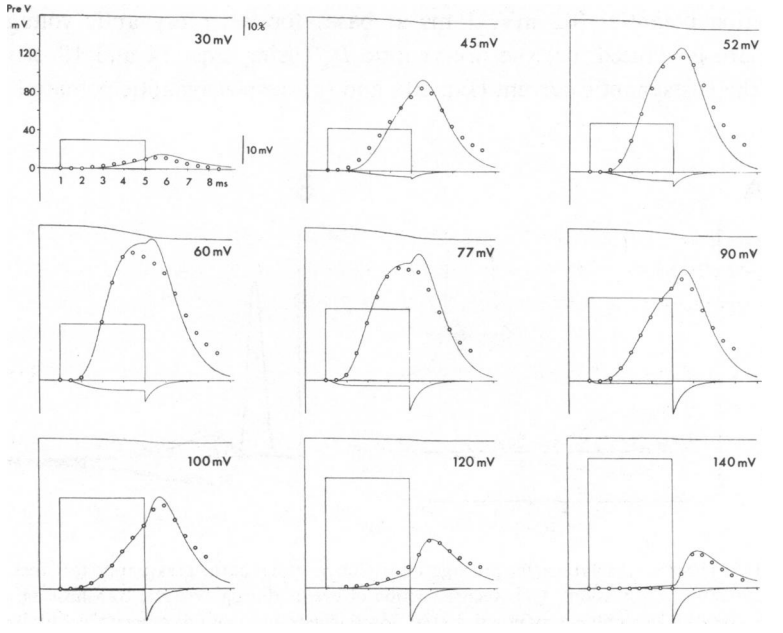

FIGURE 12 Numerical solution for mathematical model of synaptic transmission. Top trace, transmitter depletion; second trace, presynaptic voltage clamp pulse; third trace, postsynaptic response; bottom trace, calcium current. (O) recorded EPSP. $[Ca^{2+}]_o = 10$ mM.

The following points are worth noting. First, the rate constant controlling the rate of fusion of the vesicles with the membrane was found to fit the data only if it was made voltage-dependent (Fig. 10), its values dropping continuously from rest to high depolarization (i.e., fusion is affected by the magnitude of the electric field in the membrane). Furthermore, the amplitude for the "off" EPSP was also voltage-dependent, indicating that the effect of the voltage on k_f does not decay immediately after removal of the electric field but that, after a voltage clamp pulse of 4 ms, fusion rates are depressed. Second, the rate constants k_a, k_b, and k_i are also voltage-dependent suggesting that fpf may be membrane bound. Unlike k_f, these constants always returned to the same value after the clamp. Thus, the model uses the values at 0 mV depolarization for the rate constants in generating the "off" EPSP. The dependence of the various rate constants on the electric field can be understood in terms of a change in the energy of activation of the respective reactions with a change in the field.

Reconstruction of Events following a Presynaptic Action Potential

The description of the relation between calcium current and postsynaptic potential provided by the model is of further interest if it can predict the events triggered by an actual presynaptic action potential and if it can give a quantitative description of the time course and magnitude of these predicted events. Thus, the calcium current generated by an action potential as well as a voltage clamp pulse was described in our original publication (Llinás et al., 1976).

Utilizing the present more detailed model, we find that the predictions in our first publication were basically correct. Indeed, as seen in Fig. 13 *A*, following the numerical solution for Eq. 18 in the preceding paper (Llinás et al., 1981), and utilizing an experimentally recorded action potential (82 mV, 1 ms at base) for the presynaptic voltage step, three parameters are generated: (*a*) the presynaptic I_{Ca} (using Eqs. 14 and 18 of the preceding paper); (*b*) the postsynaptic current (Eq. 10); and (*c*) the postsynaptic potential (Eq. 11). The

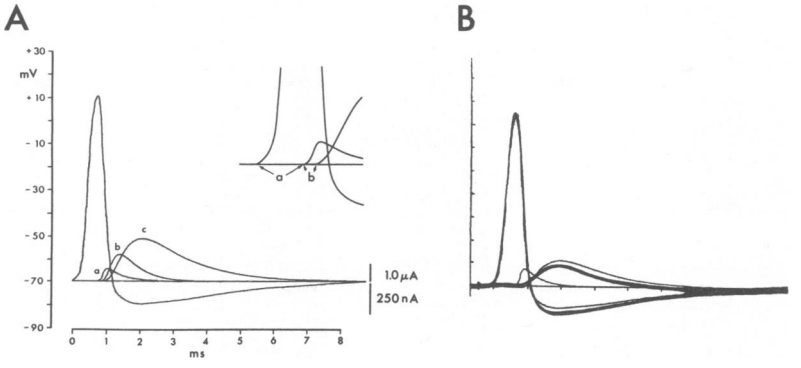

FIGURE 13 Theoretical solutions for propagating action potential in the presynaptic terminal and related steps in synaptic transmission. (*A*) Reconstruction of events during synaptic transmission: *a*, Calcium current; *b*, synaptic current; *c*, synaptic potential. Insert illustrates *a* and *b* components of synaptic delay. (*B*) Comparison of numerical solution and experimentally observed synaptic transmission. Fine lines: presynaptic action potential plus calculated I_{Ca}, and EPSP. Heavy lines: actual recording of pre- and postsynaptic response from synapse. Note that the calcium current has a late onset, and a rather prolonged time course. $[Ca^{2+}]_o$ = 10 mM.

latency of onset of I_{Ca} from the rising phase of the action potential extrapolated to baseline is ~800 μs, and close to 200-μs elapses between the onset of I_{Ca} and the onset of the postsynaptic current. The peak values for I_{Ca} calibrated from the voltage clamp measurements are ~125 nA while the postsynaptic current (1.8 nA) compares well with that experimentally measured from postsynaptic voltage clamp data (Takeuchi and Takeuchi, 1962; Llinás et al., 1974). In Fig. 13 *B* the action potential used in the model, presynaptic current, and postsynaptic potential are compared by superposition with experimentally obtained presynaptic spike and the resultant EPSP, demonstrating a reasonable fit between experimentally obtained data and that generated by the mathematical model. In this case the amplitude of the presynaptic spike was 75 mV which produced a smaller EPSP than that of the model at *A*. The calcium current generated by the model is characterized by a fast rate of rise, a slow decay, and a latency which represents most of the synaptic delay (800 μs)—the so-called *a* component; while the *b* component is, as expected, ~200 μs (insert, Fig. 13 *A*).

The relationship between amplitude and duration of the action potential and the presynaptic current and postsynaptic response is shown in Fig. 14. The records in the upper four panels illustrate the change in amplitude and time course of the presynaptic calcium current and postsynaptic potential after a change in the duration of the presynaptic action potential from 0.75 to 2 ms. The computed results suggest that the latency of the calcium

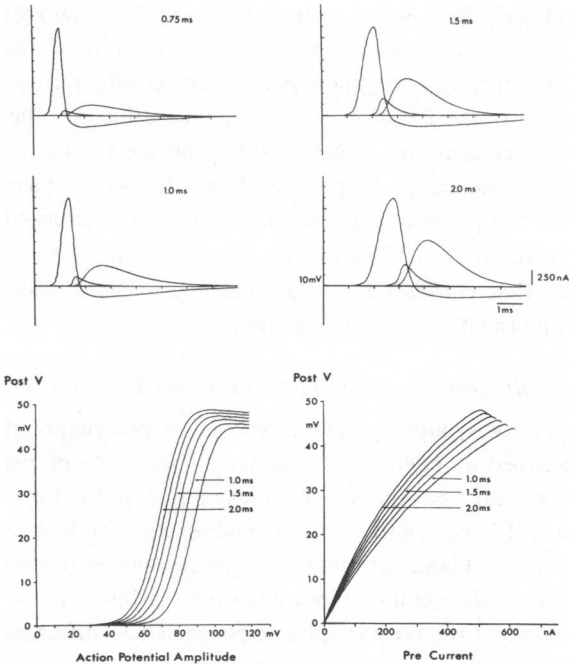

FIGURE 14 Relationship between the amplitude and duration of the presynaptic action potential, and the different variables in synaptic transmission. Top traces: presynaptic action potential, presynaptic calcium current (I_{Ca}),, and postsynaptic response (EPSP) for action potentials of different durations (durations shown to the right of each figure). Bottom left: plot of EPSP amplitude as a function of action potential amplitude for six different durations. Bottom right: plot of EPSP amplitude as a function of presynaptic current for an 80-mV action potential at different durations. $[Ca^{2+}]_o$ = 10.

current, and thus the synaptic delay, increases with the duration of the spike, as does the magnitude of the EPSP. This latter point is illustrated in the plots in the lower part of the figure where postsynaptic potential is plotted against the amplitude of the spike and against the peak pre-I_{Ca} for action potentials of various durations. The results further illustrate a rather steep relation between amplitude of the presynaptic spike and that of the EPSP and indicates that beyond a certain amplitude the action potential should cease to release more transmitter given the same resting level. Note that the relationship between I_{Ca} generated by a presynaptic spike and the postsynaptic potential is not linear, the plots curving slightly downward. The difference between the size of the EPSP and the peak I_{Ca} for different spike durations relates to the time course of I_{Ca}. Thus, for prolonged action potentials, I_{Ca} is also prolonged. The values for k_a, k_b and k_i were determined by the peak of the action potential (i.e., the same values were used for an 80-mV action potential as for an 80-mV square pulse). The value for k_f differed. Thus, in triggering transmitter release following an action potential, the rate constant for the "off" vesicle fusion (k_f) was not dependent on the action potential amplitude, but assumed the value appropriate to the resting membrane potential (the intercept value [arrow] for k_f on the plot of Pre V vs. k_f, see Fig. 10).

DISCUSSION

The present data and the model derived from them have provided a working hypothesis regarding the steps in the chain of events underlying synaptic transmission. The analysis of the voltage-dependent calcium conductance and the relationship of the calcium current to postsynaptic potentials represent the main parameters considered in this study. However, while I_{Ca} and its relation to the EPSP may be closely described by the present model, many steps in the synaptic sequence are not understood beyond the kinetics which govern the time-, voltage-, or calcium-dependence of the process. Nevertheless, because the present model is capable of reproducing and predicting several of the functional properties of this synapse, we consider it a useful heuristic tool. Taking the events which lead to synaptic transmission sequentially, we must first consider the relationship between a voltage-clamp presynaptic depolarization pulse and the postsynaptic response.

Presynaptic Voltage-Clamp Depolarization and Transmitter Release

As can be seen in Fig. 2, the synaptic potentials evoked by presynaptic depolarizations of 4 ms duration may be described as having (*a*) a close-to-linear rate of rise at low voltages, (*b*) attained a peak at or near the end of the presynaptic pulse for clamps of 50–95 mV depolarization, (*c*) an "off" postsynaptic response whose amplitude is related to the amplitude and duration of the tail I_{Ca}. These data illustrate the typical results obtained throughout the present set of experiments, the main variability between different preparations relating to the amplitude and rate of rise of the postsynaptic response. These differences were probably due to the general condition of the synapses. Thus, in many synapses the rather steep rate of rise, such as seen in Fig. 2, was not observed because the presynaptic terminal was incapable of maintaining a sufficiently high level of transmitter release. In junctions having synaptic potentials >40 mV, there is in addition saturation of the postsynaptic response. This is partly due to the voltage-dependent potassium conductance change in the postfiber (Hodgkin and Huxley, 1952) and the nonlinear summation of I_{EPSP} as stated by Boyd and Martin (1956).

However, when these variables are taken into account, the results obtained fall within an acceptable range of experimental variability as indicated by the deviation from the mean.

Amplitude of Presynaptic Voltage-Clamp Pulse and Postsynaptic Response

Depolarization-release coupling has no threshold. Indeed, with very small depolarizations a small postsynaptic response may be seen (Charlton and Atwood, 1977; Llinás, 1979), indicating that transmitter release is a continuous function of presynaptic potential. This is to be expected, as I_{Ca} is itself a continuous function of potential. Given the gain used in most of our experiments, a clear postsynaptic response was generally first detected unambiguously only for presynaptic depolarizations near 20 mV. As in the case of the presynaptic calcium current, a maximum postsynaptic response was obtained with depolarizations of 60 mV from rest. Depolarization beyond this level produced a reduction in the amplitude and rate of rise of the postsynaptic potential until finally a level was obtained such that no transmitter was released during the time of the depolarization and a sharp postsynaptic response was seen at the "break" of the presynaptic voltage step. This "off" response is indeed related to the tail calcium current analyzed in the preceding paper (Llinás et al., 1981). Of interest here is the observation that the relationship between calcium current and transmitter release is close to linear, both when analyzed as peak calcium current against postsynaptic potential (Fig. 4 *B*) or as the area of calcium current (charge displacement) against the area of the postsynaptic response (Fig. 4 *C*). As mentioned above, this relationship demonstrates a saturation at depolarizations close to 60 mV which is partly due to a similar saturation in I_{Ca}^{∞} while transmitter depletion and the nonlinear properties of the postsynaptic element are contributing factors. In addition to this saturation, the hysteresis of the I_{Ca}-EPSP curve demonstrates that for a given I_{Ca}^{∞} different values can be obtained for the postsynaptic response depending on the level of depolarization of the presynaptic membrane (see Fig. 4 *A*). Some hysteresis is still seen when the total charge displacement ($\int I_{Ca} dt$) is plotted against the total postsynaptic voltage ($\int V_{post}\, dt$, not shown). This indicates that parameters other than $[Ca^{2+}]_i$ can modulate calcium-dependent transmitter release. Indeed, as indicated in Fig. 10, the potential across the presynaptic membrane seems to regulate the effectiveness of calcium-mediated vesicle fusion and, thus, the amount of transmitter released by a given presynaptic depolarization. In fact, the hysteresis observed in Fig. 4 *A* can be explained in terms of the relative values for k_a, k_b, k_i and k_f at different values of presynaptic depolarization (Eqs. 3 and 6). The relationship between calcium current and transmitter release continues to be prominent, especially since this close-to-linear relationship is equally clear for the tail calcium current and "off" postsynaptic response (Fig. 7). As will be considered later, this set of findings indicates the limitations of relating $[Ca^{2+}]_o$ to transmitter release by any single step scheme.

Duration of Presynaptic Depolarization and Transmitter Release

Our experimental results and those of the model indicate that synaptic transmitter release is dependent on the duration, as well as the amplitude, of the presynaptic depolariztion. Voltage-clamp pulses of constant amplitude but of increasing duration produce a steady increase in the amplitude of the postsynaptic response whose rate of rise is constant for pulses having a duration $\gtrsim$1.5 ms (Fig. 5).

The steep relation between duration and transmitter release is not only of interest in establishing the properties of synaptic transmission in squid but must be taken into account

when drugs such as 3- or 4-AmP are utilized to study synaptic transmission. For instance, the addition of 1 mM 4-AmP is reported to increase the amplitude of the postsynaptic response at the neuromuscular junction by a factor of 50 at 10 mM $[Ca^{2+}]_o$ (Heuser et al., 1978). This increase is in keeping with our findings since, in the light of the present results, 3- and 4-AmP would increase calcium flux by increasing the duration of the presynaptic action potential and, in addition, probably by producing self-regenerating calcium spikes. Thus, in addition to the change in presynaptic and postsynaptic membrane resistance produced by this drug (it blocks delayed rectification), the increase in the amplitude of the postsynaptic response can be related to an increased duration and amplitude of I_{Ca}.

Transmitter Depletion

As mentioned above, transmitter depletion seems to play an important role in the functional properties of the synapse. Study of long presynaptic voltage steps clearly indicates that the squid synapse is incapable of maintaining a high level of synaptic release for periods beyond 3 or 4 ms although I_{Ca}^{∞} does not diminish. Thus, as illustrated in Fig. 6, if a depolarization of 45 mV is given for a duration of 40 ms, the postsynaptic response falls, while the level of calcium current remains stable. Because the decay is close to exponential, we may assume that it represents a true depletion from an immediately available vesicular store. The presence of depletion is not a surprising finding here as it is well known that transmission at the squid giant synapse is phasic (cf. Kusano and Landau, 1975). Indeed, during the normal life of the animal, synaptic transmission occurs with brief presynaptic action potentials and is usually utilized in short bursts (Young, 1939). This is in contrast to the more tonic synapses such as those found, for instance, in the retina (Dowling, 1970) or in the crab ganglion (Blight and Llinás, 1980) where presynaptic depolarizations can be maintained for a period of seconds without demonstrating significant decrease in postsynaptic response.

Relationship between Intracellular Calcium and Transmitter Release and Its Possible Voltage Dependence

As derived from Eq. 5, $[Ca^{2+}]_i$ near the plasma membrane follows I_{Ca} quite closely. Given this conclusion, it would be expected that the rate of transmitter release, if linearly related to $[Ca^{2+}]_i$, would be proportional in a one-to-one manner to the calcium current regardless of the level of presynaptic depolarization. However, the data in Fig. 2 and the curve in Fig. 4 *A* indicate a marked voltage-dependence of the release when moving from small to large presynaptic depolarizations. This voltage dependence is very much the same even if the sequences of measurement at different potentials are randomized. Apparently, then, the differences between calcium current and transmitter release at different potentials are related to an increased effectiveness of the intracellular calcium as the membrane field potential is modified in the depolarizing direction. The rate constants k_a, k_b, k_i, and k_f depend on the potential of the presynaptic membrane (see Fig. 10). The first three relate to processes involving fpf, suggesting that this factor is associated with the plasma membrane. A reaction rate constant may depend on electric field strength if the charge distribution of the reactants change as they go through the kinetic transition state, which may be the case with fpf. The fusion reaction characterized by k_f probably involves rearrangement of the lipids in the plasma membrane and in the vesicles. This effect on vesicle fusion seems to outlast the duration of the potential (at least for voltage clamp pulses as long as 4 ms), indicating a

certain time course for the decay of the field effect. (Note that the voltage dependence of transmitter release is not determined by a single rate constant but by the interaction of all four.) The effect of the electric field across the membrane can also be seen with the model (as shown by the solid lines in Fig. 4 *A*), suggesting an overall facilitatory effect of depolarization on the calcium-protein interaction. The exact nature of this interaction, or for that matter the precise step or steps involved in this voltage dependence of calcium-release coupling requires further study.

Synaptic Delay

One of the revealing findings in this study has been the demonstration that synaptic delay is sharply decreased when transmitter release is triggered by the tail I_{Ca}. Thus, as shown in Fig. 8 *A*, the synaptic delay for the "on" release is close to 730 ms. However, in the same synapse the "off" response showed a delay close to 200 μs (also see histogram in Fig. 8 *E*). This indicates that, as discussed in previous papers (Llinás, 1977; Llinás et al., 1979), the synaptic delay must consist of two parts: one (*a*) which relates to the time dependence of the calcium channel opening and a second (*b*) which is determined by the time required for the events which follow the entry of calcium. During a voltage clamp pulse, the 1-ms latency for the "on" postsynaptic response would be composed of both the *a* and *b* components. The shorter 200-μs latency for the "off" response would be dictated by the *b* component alone. As discussed previously, these findings immediately imply that transmitter release must take place quite close to the site of calcium entry. Indeed, as suggested by Reese (Llinás and Heuser, 1977), it is possible that the transmembrane particles seen at the active zone in the neuromuscular junction and more recently in the squid synapse (Pumplin and Reese, 1978), given their close proximity to synaptic vesicles, may in fact represent calcium channels (Pumplin et al., 1979). As expressed in the preceding paper (Llinás et al., 1981), it is very tempting to suppose that such channels are composed of a certain number of subunits (4–6). In this case then, the sequence of events relating synaptic transmission during the "on" and "off" portions of the voltage clamp would mean that while the "on" release has a delay of ~1 ms, this is mainly governed by the time dependence of the opening of the calcium channel (which, from measurement of the tail currents, has a time constant close to 600 μs), the onset of the tail current being basically instantaneous. The latter *b* latency would then give the most accurate measurement of the time between calcium influx and transmitter release.

Another important point to consider here is in reference to the voltage dependence of the latency. Indeed, while with large depolarizations the latency of the current becomes shorter (see Figs. 8 and 9 in the preceding paper), the latency of the postresponse increases. Given that synaptic delay is modulated both by the time dependence of the calcium entry and by the effect of the field across the membrane on the rate constants for the release kinetics (Fig. 8, Llinás et al., 1981), the delay does tend to increase at voltage steps above 70 mV from rest. At these voltages the rate constants for the release kinetics and not those governing I_{Ca} are the limiting factor. Thus, in considering synaptic delay, one must also take into account the effects of transmembrane electric fields.

Synaptic Release and Extracellular Calcium Concentration

One of the more studied relationships in synaptic transmission is that of extracellular calcium to transmitter release (cf. Rahamimoff et al., 1978). This has been motivated by the necessity

of understanding the calcium dependence of transmitter release in synapses where direct measurement of I_{Ca} has been, for practical reasons, impossible. Our present results indicate that transmitter release is close to linearly related to calcium current. However, as shown in our model (see Eqs. 1–3, 6–9; and Fig. 9 *B*), the relationship between calcium concentration and postsynaptic response is not simple, i.e., even the most elementary model must consider more than one presynaptic step. For this reason, attempting to extrapolate the mechanism of synaptic transmitter release from study of the relationship between $[Ca^{2+}]_o$ and postsynaptic response may in fact be rather difficult and the results obtained probably not as significant as first construed. Indeed, in this model, for $[Ca^{2+}]_o$ of 1–10 mM, the relationship between calcium concentration and postsynaptic response is exponential (Fig. 9). (Above 10 mM both the calcium current and the postsynaptic response begin to saturate.) This is the case even though here the relationship between calcium current and vesicle fusion is linear as is the relationship between I_{Ca} and EPSP amplitude (Fig. 4 *B*). This indicates that the relation between $[Ca^{2+}]_o$ and postsynaptic response is not straightforward and may not reflect that between $[Ca^{2+}]_i$ and transmitter release. Although, as shown in Figs. 3 *A–B* and 9 *A*, our experimental results and those given by the model for 3 and 10 mM $[Ca^{2+}]_o$ agree quite well, this relationship requires further, careful, study.

This is especially true in the light of other studies of the dependence of transmitter release on external calcium in this preparation. Katz and Miledi (1970) reported an ~2.5 power relationship between $[Ca^{2+}]_o$ and EPSP amplitude for calcium concentrations of 2.75–11 mM. They point out that "this power index can vary considerably in different experiments, and that transmitter release following a nerve impulse may increase with as much as the fourth or even higher power of $[Ca^{2+}]_o$". Lester (1970) reported a maximum power relation of 3.39 for concentrations of 0.9–4.6 mM; however, if the data in Fig. 7 of Kusano (1970) is plotted as log $[Ca^{2+}]_o$ vs. log EPSP amplitude, a maximum power relation of 1.28 is found for a 60 mV pulse.

The absence of a fourth power relationship between $[Ca^{2+}]_o$ and postsynaptic response in this synapse could be considered at variance with results obtained at the neuromuscular junction. However, given the sigmoidal relationship between $[Ca^{2+}]_o$ and postsynaptic response below 1 mM (Dodge and Rahamimoff, 1967), a close-to-linear range between these two variables is expected at $[Ca^{2+}]_o$ above this value and, thus, no discrepancy may actually exist.

Finally, it must be emphasized that, given the steep relation between the amplitude and duration of the presynaptic voltage and I_{Ca}, experiments based on presynaptic action potentials are subject to a multitude of variables quite difficult to control or quantify. Thus, even in such cases where a presynaptic action potential is recorded, small changes in its duration, rate of rise, and especially rate of fall, and/or amplitude, may generate a large variation in the EPSP amplitude.

A Model for Synaptic Transmission

Any model that attempts to relate the postsynaptic response to the presynaptic calcium influx has to assume a plausible relationship between the $[Ca^{2+}]_i$ and its effectiveness in promoting vesicle fusion with the plasma membrane. The specificity of calcium in triggering release of transmitter led us to assume that the presynapse has an fpf which can bind calcium

specifically and which facilitates vesicle fusion upon binding. A simple scheme has thus been proposed for the binding of calcium to the fpf and for the activation and inactivation of the complex formed.

Another consideration that must be included in the proposed model is the concentration of vesicles at the plasma membrane. For the sake of simplicity, it was assumed that the rate of fusion is proportional to the number of vesicles available at the synaptic site, and a depletion parameter, based on the rate of fall of EPSPs during long voltage clamp pulses, has been included.

In the chain of events between the entry of calcium into the presynaptic terminal and the postsynaptic response, a few steps need consideration. The $[Ca^{2+}]_i$ was assumed to be proportional to the calcium influx with a negligible delay and to persist beyond the duration of the depolarization. The formal justification for neglecting the delay has been presented, its physical basis being the small dimensions (~1,500 Å diam) of the alleged source of I_{Ca}—the patch of membrane particles as visualized by freeze etching (Pumplin and Reese, 1978). A specific term for calcium binding or sequestering within the presynaptic terminal has not been included in this model as very little quantitative information concerning this process is available. However, the low diffusion constant for cytoplasmic calcium diffusion and a pathway for inactivation without prior activation of the fpf · Ca^{2+} complex is analogous to such a process. Another link in the chain of events is the diffusion of the transmitter across the synaptic cleft. This is readily shown to be in the microsecond range and is, therefore, not significant in this case. Lastly, the response of the postsynaptic receptor to the transmitter must be considered. In the absence of data concerning the receptor in this synapse, both opening and closing were assumed to follow first-order kinetics; this seems to be a reasonable approximation in light of knowledge of other well studied receptors (Magleby and Stevens, 1972; Neher and Stevens, 1979) and permits an acceptable fit of the model to the experimental findings.

The experimental results were obtained at the Marine Biological Laboratory in Woods Hole, Mass. Mr. Michio Chujo was of invaluable help in writing the computer programs and obtaining the numerical solutions. Research was supported by U. S. Public Health Service grants NS-13742 and NS-14014 from the National Institute of Neurological and Communicative Disorders and Stroke.

Received for publication 15 October 1980.

REFERENCES

ALEMA, S., P. CALISSANO, G. RUSCA and A. GIUDITTA. 1973. Identification of a calcium-binding, brain-specific, protein in the axoplasm of squid giant axons. *J. Neurochem.* **20**:681–689.

ARMSTRONG, C. M., and L. BINSTOCK. 1965. Anomalous rectification in the squid giant axon injected with tetraethylammonium chloride. *J. Gen. Physiol.* **48**:859–872.

BAKER, P. F. 1972. Transport and metabolism of calcium ions in nerve. *Prog. Biophys. Molec. Biol.* **24**:177–223.

BAKER, P. F., A. L. HODGKIN, and E. B. RIDGWAY. 1971. Depolarization and calcium entry in squid giant axons. *J. Physiol. (Lond.).* **218**:709–755.

BAKER, P. F., and W. W. SCHAEPFER. 1978. Uptake and binding of calcium by axoplasm isolated from giant axons of *Loligo* and *Myxicola*. *J. Physiol. (Lond.).* **276**:103–125.

BLAUSTEIN, M. P., R. W. RATZLAFF, and N. C. KENDRICK. 1978 *a*. The regulation of intracellular calcium in presynaptic nerve terminals. *Ann. N. Y. Acad. Sci.* **307**:195–212.

BLAUSTEIN, M. P., R. W. RATZLAFF, N. C. KENDRICK, and E. S. SCHWEITZER. 1978 *b*. Calcium buffering in presynaptic nerve terminals. I. Evidence for involvement of a nonmitochondrial ATP-dependent sequestration mechanism. *J. Gen. Physiol.* **72**:15–41.

BLAUSTEIN, M. P., R. W. RATZLAFF, and E. S. SCHWEITZER. 1978 *c*. Calcium buffering in presynaptic nerve terminals. II. Kinetic properties of the nonmitochondrial Ca sequestration mechanism. *J. Gen. Physiol.* **72**:43–66.

BLIGHT, A. R., and R. LLINÁS. 1980. The non-impulsive stretch-receptor complex of the crab: a study of depolarization-release coupling at a tonic sensorimotor synapse. *Phil. Trans. R. Soc. Lond. B Biol. Sci.* **290**:219–276.

BLOEDEL, J. R., P. W. GAGE, R. LLINÁS, and D. M. J. QUASTEL. 1966. Transmitter release at the squid giant synapse in the presence of tetrodotoxin. *Nature (Lond.).* **212**:49–50.

BOYD, I. A., and A. R. MARTIN. 1956. The end-plate potential in mammalian muscle. *J. Physiol. (Lond.).* **132**:74–91.

BRYANT, S. H. 1958. Transmission in squid giant synapses. The importance of oxygen supply and the effects of drugs. *J. Gen. Physiol.* **41**:473–484.

BULLOCK, T. H. 1948. Properties of a single synapse in the stellate ganglion of squid. *J. Neurophysiol.* **11**:343–364.

BULLOCK, T. H., and S. HAGIWARA. 1957 Intracellular recording from the giant synapse of the squid. *J. Gen. Physiol.* **40**:565–577.

CARSLAW, H. S., and J. C. JAEGER. 1959. Conduction of Heat in Solids, 2nd Ed. Clarendon Press, Oxford.

CHARLTON, M. P., and H. L. ATWOOD. 1977. Slow release of transmitter at the squid giant synapse. *Neurosci. Lett.* **5**:165–196.

DODGE, F. A., and R. RAHAMIMOFF. 1967. Cooperative action of calcium ions in transmitter release at the nuclear junction. *J. Physiol. (Lond.).* **193**:419–432.

DOWLING, J. E. 1970. Organization of vertebrate retinas. *Invest. Ophthalmol.* **9**:655–8680.

HAGIWARA, S., and I. TASAKI. 1958. A study on the mechanism of impulse transmission across the giant synapse of the squid. *J. Physiol. (Lond.).* **143**:114–137.

HEUSER, J. E., T. S. REESE, M. J. DENNIS, Y. JAN, and L. JAN. 1979. Exocytosis of synaptic vesicles captured by quick freezing. *J. Cell Biol.* **81**:275–300.

HODGKIN, A. L., and A. F. HUXLEY. 1952. The components of membrane conductance in the giant axon of *Loligo*. *J. Physiol. (Lond.).* **116**:473–496.

HODGKIN, A. L., and R. D. KEYNES. 1957. Movements of labelled calcium in squid giant axon. *J. Physiol. (Lond.).* **138**:253–281.

KATZ, B. 1969. The Release of Neural Transmitter Substances. Sherrington Lecture X. Charles C. Thomas, Springfield, Ill.

KATZ, B., and R. MILEDI. 1967. A study of synaptic transmission in the absence of nerve impulses. *J. Physiol. (Lond.).* **192**:407–436.

KATZ, B., and R. MILEDI. 1969 *a*. Tetrodotoxin-resistant electric activity in presynaptic terminals. *J. Physiol. (Lond.).* **203**:459–487.

KATZ, B., and R. MILEDI. 1969 *b*. The effect of divalent cations on transmission in the squid giant synapse. *Publ. Staz. Zool. Napoli.* **37**:303–310.

KATZ, B., and R. MILEDI. 1970. Further study of the role of calcium on synaptic transmission. *J. Physiol. (Lond.).* **207**:789–801.

KATZ, B., and R. MILEDI. 1971. The effect of prolonged depolarization on synaptic transfer in the stellate ganglion of the squid. *J. Physiol. (Lond.).* **216**:503–512.

KELLY, R. B., J. W. DEUTSCH, S. S. CARLSON, and J. A. WAGNER. 1979. Biochemistry of neurotransmitter release. *Ann. Rev. Neurosci.* **2**: 339–446.

KUSANO, K. 1968. Further study of the relationship between pre- and postsynaptic potentials in the squid giant synapse. *J. Gen. Physiol.* **52**: 326–345.

KUSANO, K. 1970. Influence of ionic environment on the relationship between pre- and postsynaptic potentials. *J. Neurobiol.* **1**:435–457.

KUSANO, K., and E. M. LANDAU. 1975. Depression and recovery of transmission at the giant synapse. *J. Physiol. (Lond.)* **245**:13–32.

KUSANO, K., D. R. LIVENGOOD, and R. WERMAN. 1967. Correlation of transmitter release with membrane properties of the presynaptic fiber of the squid giant synapse. *J. Gen. Physiol.* **50**:2579–2601.

LESTER, H. A. 1970. Transmitter release by presynaptic impulses in the squid stellate ganglion. *Nature (Lond.).* **227**:493–496.

LLINÁS, R. 1977. Calcium and transmitter release in squid synapse. *Soc. Neurosci. Symp.* **2**:139–160.

LLINÁS, R. 1979. The role of calcium in neuronal function. *In* The Neurosciences: Fourth Study Program. F. O. Schmitt, and F. G. Worden, editors. M.I.T. Press, Cambridge. 555–571.

LLINÁS, R., and J. R. HEUSER. 1977. Depolarization-release coupling systems in neurons. *Neurosci. Res. Prog. Bull.* **15**:557–687.

LLINÁS, R., R. W. JOYNER, and C. NICHOLSON. 1974. Equilibrium potential for the postsynaptic response in the squid giant synapse. *J. Gen. Physiol.* **64**:519–535.

LLINÁS, R., and C. NICHOLSON. 1975. Calcium role in depolarization-secretion coupling: an aequorin study in squid giant synapse. *Proc. Natl. Acad. Sci. U.S.A.* **72**:187–190.

LLINÁS, R., I. Z. STEINBERG, and K. WALTON. 1976. Presynaptic calcium currents and their relation to synaptic transmission: voltage clamp study in squid giant synapse, and theoretical model for the calcium gate. *Proc. Natl. Acad. Sci. U.S.A.* **73**:2918–2922.

LLINÁS, R., I. Z. STEINBERG, and K. WALTON. 1979. A model for synaptic transmission. *Brain Res. Bull.* **4**:170–173.

LLINÁS, R., I. Z. STEINBERG, and K. WALTON. 1981. Presynaptic calcium currents in squid giant synapse. *Biophys. J.* **33**:289–322.

LLINÁS, R., K. WALTON, and V. BOHR. 1976. Synaptic transmission in squid giant synapse after potassium conductance blockage with external 3-, and 4-aminopyridine. *Biophys. J.* **16**:83–86.

MAGLEBY, K. L., and C. F. STEVENS. 1972. A quantitative description of end-plate currents. *J. Physiol. (Lond.).* **223**:173–197.

MEVES, H., and Y. PICHON. 1977. The effect of internal and external 4-aminopyridine on the potassium currents in intracellularly perfused squid giant axons. *J. Physiol. (Lond.).* **268**:511–532.

MILEDI, R., and C. R. SLATER. 1966. The action of calcium on neuronal synapses in the squid. *J. Physiol. (Lond.)* **184**:473–498.

NARAHASHI, T., J. W. MOORE, and W. R. SCOTT. 1964. Tetrodotoxin blockage of sodium conductance increase on lobster giant axons. *J. Gen. Physiol.* **47**:965–974.

NEHER, E., and D. F. STEVENS. 1979. Voltage-driven conformational changes in intrinsic membrane proteins. *In* The Neurosciences: Fourth Study Program. F. O. Schmitt and F. G. Worden, editors. M.I.T. Press, Cambridge, Mass. 623–629.

PARSEGIAN, V. A. 1977. Considerations in determining the mode of influence of calcium on vesicle-membrane interaction. *Soc. Neurosci. Symp.* **2**:161–171.

PELHATE, M., and Y. PICHON. 1974. Selective inhibition of potassium current in giant axon of cockroach. *J. Physiol. (Lond.).* **242**:P90–91.

PUMPLIN, D. W., and T. S. REESE. 1978. Membrane ultrastructure of the giant synapse of the squid *Loligo pealei*. *Neuroscience.* **3**:685–696.

PUMPLIN, D. W., R. LLINÁS, and T. S. REESE. 1979. Morphological parameters of the squid giánt synapse: relationship of active zone particles to ionic conductance. *Soc. Neurosci. Abst.* **5**:259.

RAHAMIMOFF, R., S. D. ERULKAR, A. LEV-TOV, and H. MEIRI. 1978. Intracellular and extracellular calcium ions in transmitter release at the neuromuscular synapse. *Ann. N. Y. Acad. Sci.* **307**:583–589.

SHAPIRO, E., V. F. CASTELLUCCI, and E. R. KANDEL. 1980. Presynaptic membrane potential affects transmitter release in an identified neuron in Aplysia by modulating the Ca^{2+}, and K^+ currents. *Proc. Natl. Acad. Sci. U.S.A.* **77**:629–633.

STEINBACH, J. H., and C. F. STEVENS. 1976. Neuromuscular transmission. *In* Frog Neurobiology: A Handbook. R. Llinás, and W. Precht, editors. Springer-Verlag, New York. 33–92.

TAKEUCHI, A., and N. TAKEUCHI. 1962. Electrical changes in pre- and postsynaptic axons of the giant synapse of *Loligo*. *J. Gen. Physiol.* **45**:1181–1193.

YEH, J. Z., G. S. OXFORD, C. H. WU, and T. NARAHASHI. 1976. Dynamics of aminopyridine block of potassium channels in squid axon membrane. *J. Gen. Physiol.* **68**:519–535.

YOUNG, J. Z. 1939. Fused neurons and synaptic contacts in the giant nerve fibres of cephalopods. *Philos. Trans. R. Soc. Lond. B Biol. Sci.* **229**:465–503.